

## Quality of Long LSO/LYSO Crystals

This article has been downloaded from IOPscience. Please scroll down to see the full text article.

2012 J. Phys.: Conf. Ser. 404 012026

(<http://iopscience.iop.org/1742-6596/404/1/012026>)

View [the table of contents for this issue](#), or go to the [journal homepage](#) for more

Download details:

IP Address: 131.215.71.79

The article was downloaded on 14/03/2013 at 15:18

Please note that [terms and conditions apply](#).

# Quality of Long LSO/LYSO Crystals

**Ren-Yuan Zhu**

256-48, HEP, Caltech, Pasadena, CA 91125, USA

E-mail: [zhu@hep.caltech.edu](mailto:zhu@hep.caltech.edu)

**Abstract.** Because of their high stopping power ( $X_0 = 1.14$  cm) and fast ( $t = 40$  ns) and bright (4 times of BGO) scintillation cerium doped silicate based heavy crystal scintillators (LSO and LYSO) have attracted a broad interest in the high energy physics community pursuing precision electromagnetic calorimeter for future high energy physics experiments. Their excellent radiation hardness against  $\gamma$ -rays, neutrons and charged hadrons also makes them a preferred material for calorimeters to be operated in a severe radiation environment, such as the HL-LHC. The optical and scintillation properties and its radiation hardness against  $\gamma$ -ray irradiations up to 1 Mrad are presented for the first  $2.5 \times 2.5 \times 28$  cm LYSO sample. An absorption band was found at the seed end of this sample and three other long samples, which was traced back to a bad seed crystal used in the corresponding crystal growth process. Significant progresses in optical and scintillation properties were achieved for large size LYSO crystals after eliminating this absorption band. Their application in future HEP experiments at HL-LHC are discussed.

## 1. Introduction

In the last two decades, cerium doped silicate based heavy crystal scintillators have been developed for the medical industry. As of today, mass production capabilities of lutetium oxyorthosilicate (LSO) [1] and lutetium-yttrium oxyorthosilicate (LYSO) [2, 3] are established. Because of their high stopping power ( $\rho = 7.4$  g/cm<sup>3</sup>,  $X_0 = 1.14$  cm and  $R_{Moliere} = 2.07$  cm), high light yield (about 4 times of BGO) and fast decay time ( $\tau = \sim 40$  ns) these crystals have also attracted a broad interest in the physics community for future high energy physics experiments [4], such as the proposed SuperB forward endcap calorimeter [5], the KLOE experiment [6] and the Mu2e experiment [7]. Investigations on large size ( $2.5 \times 2.5 \times 20$  cm) LSO/LYSO crystals also show that this new generation of inorganic crystal scintillators has excellent radiation hardness against  $\gamma$ -rays [8], neutrons [9] and charged hadrons [10]. This material thus may also be considered for calorimeters to be operated in a severe radiation environment, such as the HL-LHC, and seems the only suitable scintillator for which mass-production capability is presently available.

The main obstacles of using this material in the experimental physics are two fold: the availability of high quality crystals in sufficiently large size and the high cost associated with their raw material cost and high melting point ( $> 2,000^\circ\text{C}$ ). An effort has been made at Sichuan Institute of Piezoelectric and Acousto-optic Technology (SIPAT), Chongqing, China, to grow large size (up to 28 cm or 25  $X_0$  long) LSO and LYSO crystals for high energy physics applications. In this work, the first  $2.5 \times 2.5 \times 28$  cm LYSO sample from SIPAT is evaluated, including its optical and scintillation properties and its radiation hardness against  $\gamma$ -rays up to 1 Mrad. Poor longitudinal transmittance was observed in this sample, which was found to be caused by an absorption band at the seed end. After removing this absorption band both the

optical and scintillation properties are improved significantly for large size samples. This report is a part of an on-going R&D program to further develop this material to be of practical use at the HL-LHC.

## 2. 20 cm long LSO/LYSO Crystal Crystals

Large size LSO and LYSO crystals are routinely grown in industry [11]. Figure 1 shows four long crystal samples of  $2.5 \times 2.5 \times 20$  cm<sup>3</sup> from CTI Molecular Imaging (CTI), Crystal Photonics, Inc. (CPI), Saint-Gobain Ceramics & Plastics, Inc. (Saint-Gobain) and Sichuan Institute of Piezoelectric and Acousto-optic Technology (SIPAT). Figure 2 shows the spectra of 0.51 MeV  $\gamma$ -rays from a <sup>22</sup>Na source observed with coincidence triggers [11]. The readout devices used are a Hamamatsu R1306 PMT (Left) and two Hamamatsu S8664-55 APDs (Right). The FWHM resolution for the 0.51 MeV  $\gamma$ -ray is about 12% for the PMT readout, which can be compared to 15% for the BGO sample. With the APD readout, the  $\gamma$ -ray peaks are clearly visible. The energy equivalent readout noise was less than 40 keV for these long LSO and LYSO samples.

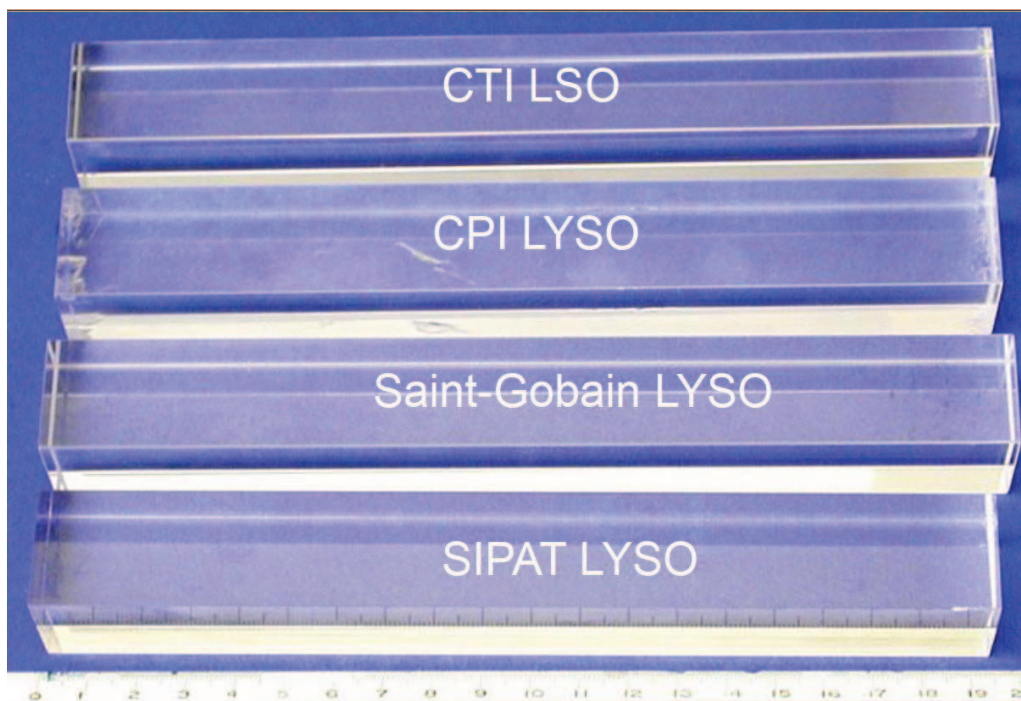


**Figure 1.** A photo shows four long crystal samples with dimension of  $2.5 \times 2.5 \times 20$  cm<sup>3</sup>.

LSO/LYSO crystals is also found to be much more radiation hard than other crystals commonly used in high energy and nuclear physics experiment, such as BGO, CsI(Tl) and PbWO<sub>4</sub> [12]. Their scintillation mechanism is not damaged by  $\gamma$ -ray irradiation. Radiation damage in LSO and LYSO crystals recovers very slow under room temperature but can be completely cured by thermal annealing at 300°C for ten hours. The energy equivalent  $\gamma$ -ray induced readout noise was estimated to be about 0.2 MeV and 1 MeV respectively in a radiation environment of 15 rad/h and 500 rad/h for LSO and LYSO samples of  $2.5 \times 2.5 \times 20$  cm<sup>3</sup> [8]. Figure 3 (Left) shows an expanded view of the longitudinal transmittance spectra for three samples before and after several steps of the  $\gamma$ -ray irradiation with integrated dose of  $10^2$ ,  $10^4$  and  $10^6$  rad. Also shown in the figure is the corresponding numerical values of the photo-luminescence weighted longitudinal transmittance (*EWLT*). Figure 3 (Right) shows the normalized average light output as a function of integrated dose for five long samples from

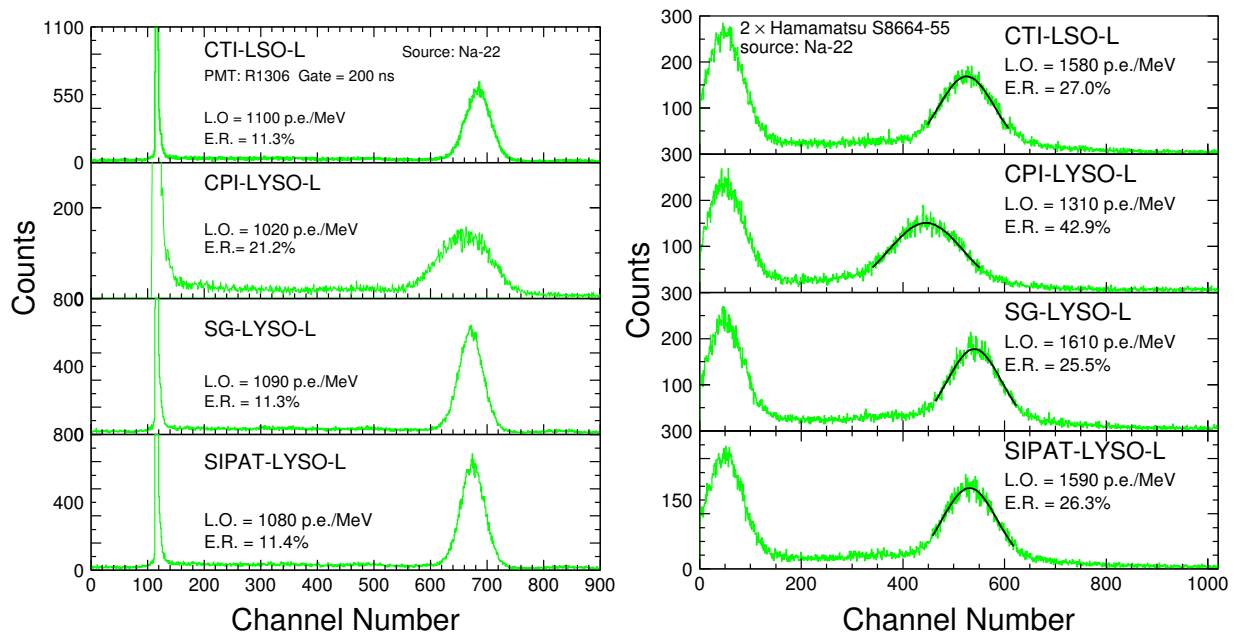


**Figure 2.** The spectra of 0.511 MeV  $\gamma$ -rays from a  $^{22}\text{Na}$  source, measured by a Hamamatsu R1306 PMT (Left) and two Hamamatsu S8664-55 APDs (Right), with a coincidence trigger for four long LSO and LYSO samples from CTI, CPI, Saint-Gobain and SIPAT.

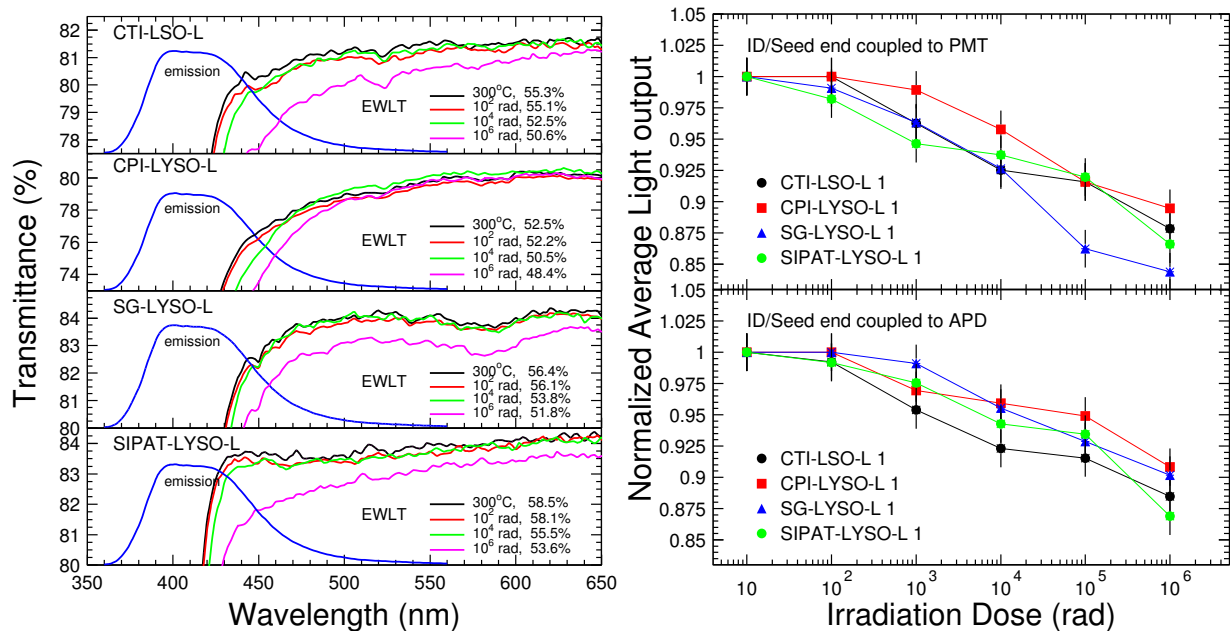


**Figure 3.** Left: The longitudinal transmittance spectra are shown as a function of wavelength in an expanded scale together with the photo-luminescence spectra for four LSO and LYSO samples before and after the irradiation with integrated doses of  $10^2$ ,  $10^4$  and  $10^6$  rad. Right: The normalized light output is shown as a function of the integration dose for four long LSO and LYSO samples with PMT (top) and APD (bottom) as the readout devices.

various vendors. It is interesting to note that all samples show consistent radiation resistance with degradations of both the light output and transmittance at 10 to 15% level after  $\gamma$ -ray irradiation with an integrated dose of 1 Mrad.

### 3. The First 28 cm long LYSO Sample

Figure 4 is a photo showing a LYSO ingot (top) and the first  $2.5 \times 2.5 \times 28$  cm LYSO sample (bottom) grown at SIPAT. The diameter of the ingot is about 60 mm and the length of the constant diameter is about 310 mm. From this ingot the first 28 cm long LYSO sample (SIPAT-LYSO-L7) was obtained.

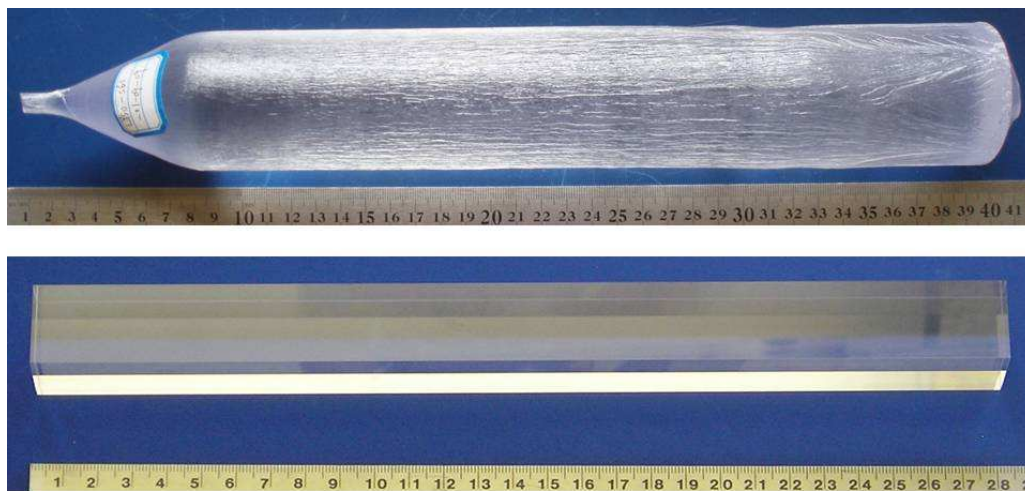


**Figure 4.** Top: A LYSO ingot grown by SIPAT with constant diameter of 60 mm and 310 mm long (top). Bottom: The first 25 X<sub>0</sub> long LYSO sample of  $25 \times 25 \times 280$  mm cut from the ingot.

All six surfaces of the sample are polished. Its dimension is found to be within  $100 \mu\text{m}$  tolerance to the nominal values. The sample is colorless, crack free, without any visible inclusion. No thermal treatment was applied before the initial measurements. According to the manufacturer, the yttrium concentration is about 7%. The nominal cerium doping level is about 0.2%. The actual cerium concentration in the sample, however, would be less than the nominal value because of the cerium segregation. The distribution of the cerium concentration along the long sample's axis is not uniform.

The UV excited photo-luminescence spectra at two ends of the sample were measured by a Hitachi F-4500 fluorescence spectrophotometer. The angle between the sample normal and the excitation beam is set to be  $10^\circ$  to avoid internal absorption of the crystal [13]. The Left plot of Figure 5 shows the excitation (dashed lines) and photo-luminescence (solid lines) spectra measured at the seed (top) and tail (bottom) end of SIPAT-LYSO-L7. Both the excitation and emission spectra are consistent between these two ends, indicating no deviation of scintillation along the crystal.

The longitudinal and transverse transmittance spectra were measured using a Perkin Elmer Lambda 950 spectrophotometer equipped with double beam, double monochromator and a general purpose optical bench (GPOB) with light path up to 40 cm. The systematic uncertainty in repeated measurements is about 0.15%.

The right plot of Figure 5 shows the longitudinal transmittance spectrum (black line) for SIPAT-LYSO-L7. Also shown in this figure are the theoretical limits of the transmittance

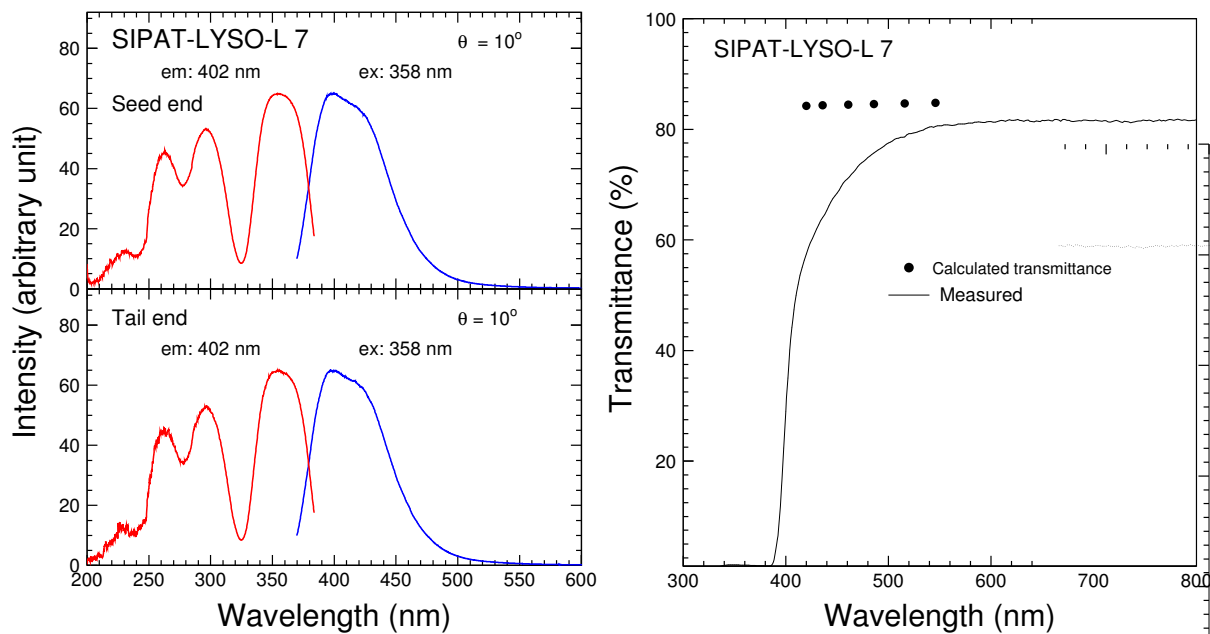


**Figure 5.** Left: The excitation (dashed lines) and photo-luminescence (solid lines) spectra are shown as a function of wavelength for SIPAT-LYSO-L7. Right: The longitudinal transmittance spectrum (black lines) is shown as a function of wavelength for SIPAT-LYSO-L7 together with the theoretical limits (black dots).

(black dots) calculated by using the refractive index of LYSO [13]. Taking into account multiple bouncing between two end surfaces the theoretical limits of the transmittance without internal absorption can be calculated as [14]

$$\begin{aligned} T_s &= (1 - R)^2 + R^2(1 - R)^2 + \dots \\ &= (1 - R)/(1 + R), \end{aligned} \quad (1)$$

where

$$R = \frac{(n_{crystal} - n_{air})^2}{(n_{crystal} + n_{air})^2}, \quad (2)$$

where  $n_{crystal}$  and  $n_{air}$  are the refractive index of crystal and air respectively, which is a function of wavelength.

A comparison of the measured optical transmittance and its theoretical limit reveals sample's overall optical quality. Poor transmittance was found between 400 nm and 600 nm. The left plot of Figure 6 shows the transverse transmittance spectra measured every 2 cm from the seed (curve-1) to the tail (curve-13) end. A large divergence of the transverse transmittance spectra between 400 and 600 nm is observed. The insert shows an expanded view between 420 nm and 450 nm, illustrating clearly the degradation of transmittance from the tail end to the seed end. While the transverse transmittance measured at 2 cm from the tail end (curve-13) is very good, that measured at 2 cm from the seed end is rather poor. From these spectra alone one can not judge if the poor transmittance observed at the seed end is caused by internal absorption or scattering. Also shown in this figure is the cut-off wavelength for the transverse transmittance. It is defined as the wavelength at which the transmittance value is 50% of the theoretical value at 600 nm. From the numerical values of the cut-off wavelength one may extract the cerium concentration by using an established correlation. This will be discussed in our future publication.



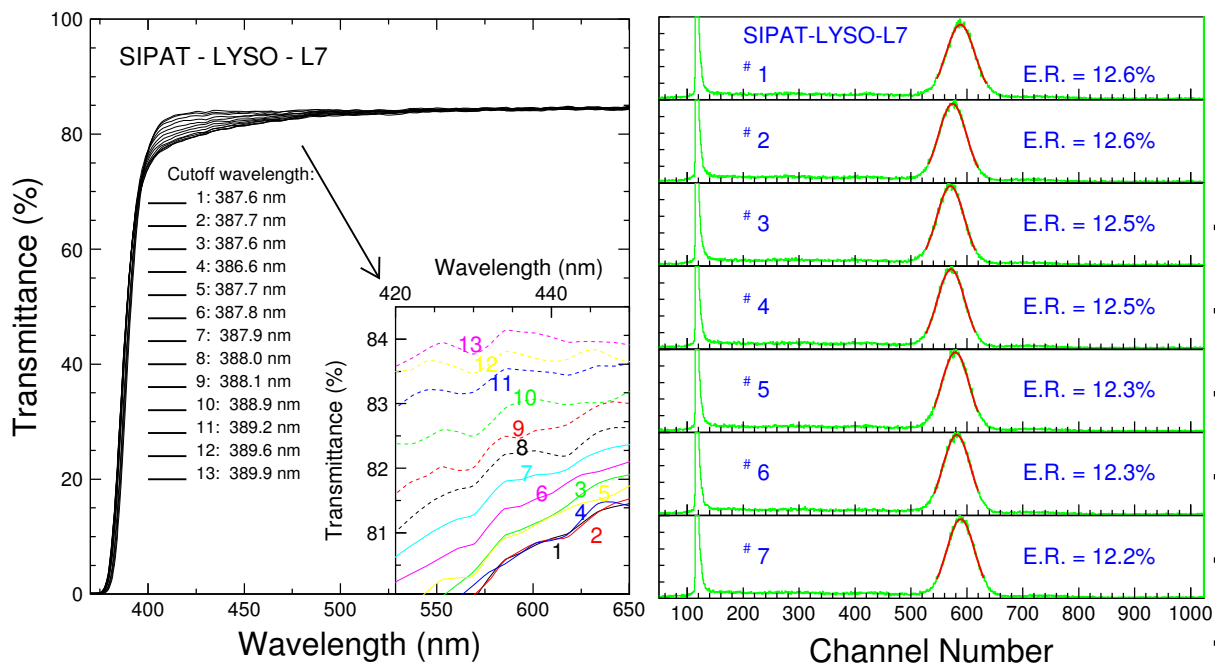


**Figure 6.** Left: The transverse transmittance spectra measured every 2 cm from the seed (curve-1) to the tail (curve-13) end are shown as a function of wavelength for SIPAT-LYSO-L7. The inset is an expanded view between 420 nm and 450 nm. Right: The pulse height spectra of 0.511 MeV  $\gamma$ -ray peaks (solid lines) and corresponding Gaussian fits measured by a Hamamatsu R1306 PMT are shown at seven points evenly distributed along SIPAT-LYSO-L7. Also shown are the numerical values of the FWHM energy resolutions (E.R.).

Despite the poor transmittance observed at the seed end this 28 cm long LYSO sample provides adequate light output and energy resolution. Two photodetectors, a Hamamatsu R1306 PMT and a Hamamatsu S8664-1010 APD with 1 cm<sup>2</sup> area, were used in the light output measurement. In these measurements the seed end of the sample was coupled to the PMT via Dow Corning 200 fluid, while all other faces of the sample were wrapped with two layers of Tyvek paper. To reduce the effect of the intrinsic natural radioactivity, a collimated <sup>22</sup>Na source was used with a coincidence trigger provided by a BaF<sub>2</sub> crystal. The detail of the setup used in these measurements is discussed in reference [4]. The  $\gamma$ -ray peak position was determined by a simple Gaussian fit. The right plot of Figure 6 shows the pulse height spectra measured by the Hamamatsu R1306 PMT at seven points evenly distributed along SIPAT-LYSO-L7. The FWHM resolutions obtained for 0.511 MeV  $\gamma$ -rays from the <sup>22</sup>Na source are about 12.5%, which is quite good for crystals of such length.

The  $\gamma$ -ray peak positions obtained by sending a collimated beam of  $\gamma$ -ray at seven points evenly distributed along the crystal were used to extract the light response uniformity of the crystal. A linear fit is used to fit the normalized response

$$\frac{LO}{LO_{mid}} = 1 + \delta \frac{x}{x_{mid} - 1}, \quad (3)$$

where  $LO_{mid}$  represents the average light output at the middle of the sample,  $x$  is the distance from the end coupled to the readout device and  $\delta$  represents the deviation of the light response uniformity.

This sample was measured with both PMT and APD readout. The average light output is 1,380 p.e./MeV and 1,510 p.e./MeV for the PMT and APD readout respectively. The

corresponding light response uniformities ( $\delta$  values) are  $0.7 \pm 1\%$  and  $2.8 \pm 1.5\%$ . Despite its poor transmittance observed at the seed end this 28 cm long LYSO sample shows rather good longitudinal light response uniformity.

#### 4. Radiation Resistance of the First 28 cm long sample against $\gamma$ -ray Irradiations

Radiation damage of this sample against  $\gamma$ -rays was investigated. A  $^{137}\text{Cs}$  source was used for the irradiations with a dose rate of 7,500 rad/h. The irradiation was carried out step by step to integrated doses of  $10^2$ ,  $10^4$  and  $10^6$  rad. Since radiation damage in LYSO crystals does not recover, and is not dose rate dependent [8], the total integrated dose is used to represent the level of the radiation applied to this sample in this study.

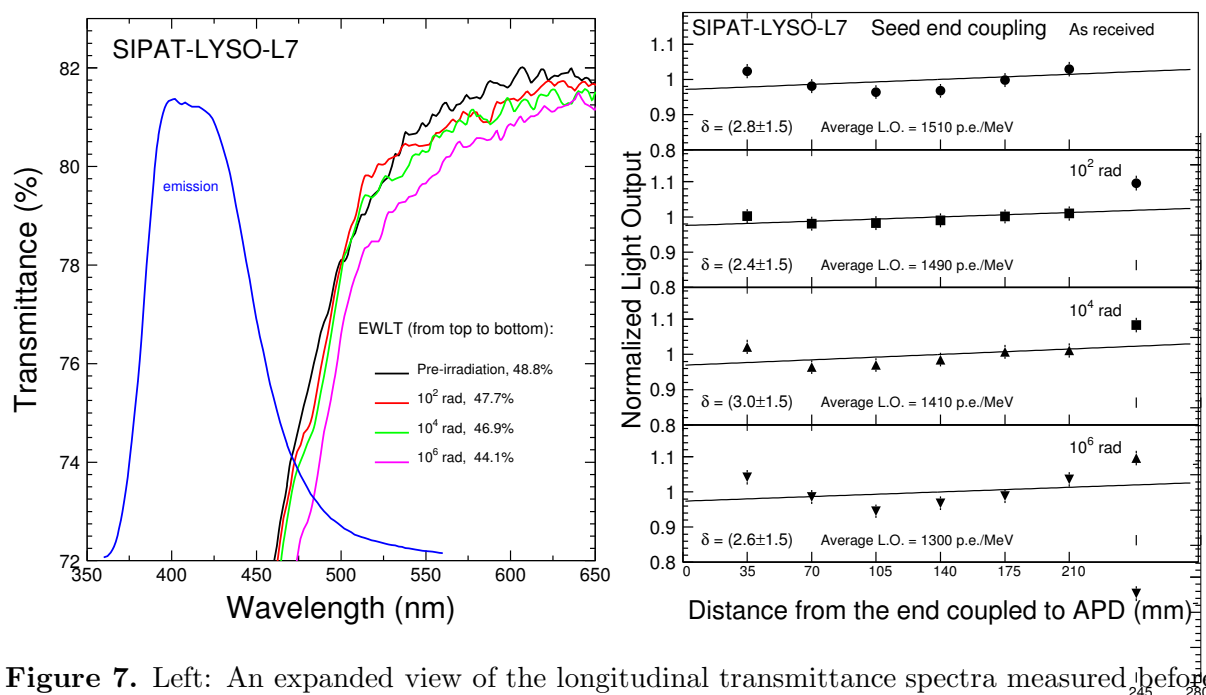


**Figure 7.** Left: An expanded view of the longitudinal transmittance spectra measured before and after  $\gamma$ -ray irradiations in several steps up to 1 Mrad is shown for SIPAT-LYSO-L7. Also shown is the emission spectrum and the values of EWLTL defined in the text. Right: Normalized light output and light response uniformity measured by Hamamatsu S8664-1010 APD before and after  $\gamma$ -ray irradiations in several steps up to 1 Mrad are shown for SIPAT-LYSO-L7.

The left plot of Figure 7 shows an expanded view of the longitudinal transmittance spectra before and after the  $\gamma$ -ray irradiations with an integrated dose of  $10^2$ ,  $10^4$  and  $10^6$  rad. Also shown in the figure is the emission spectrum and the values of the emission weighted longitudinal transmittance (EWLT), which is defined as

$$EWLT = \frac{\int LT(\lambda)Em(\lambda)d\lambda}{\int Em(\lambda)d\lambda} \quad (4)$$

The numerical value of EWLT represents how transparent the crystal is to the scintillation light so is a good measure of its transparency. Its degradation represents the radiation damage effect on transparency. For SIPAT-LYSO-L7 its radiation damage in EWLT is 9.6% after 1 Mrad irradiations.

The right plot of Figure 7 shows the normalized light output and response uniformity measured by the Hamamatsu APD before and after  $\gamma$ -ray irradiations with an integrated dose of



$10^2$ ,  $10^4$  and  $10^6$  rad. The damage on the light output was found to be about 13% after 1 Mrad irradiations. This is much better than 26% light output loss measured for typical lead tungstate (PWO) crystals after 10 krad with a dose rate of 400 rad/h [15]. We also note that the light response uniformity of SIPAT-LYSO-L7 does not change, indicating that its energy resolution may be maintained even after 1 Mrad irradiations. Despite the poor transmittance at the seed end and the radiation resistance of this 28 cm long LYSO sample SIPAT-LYSO-L7 is quite good.

### 5. Progress on Optical and Scintillation Properties in Long LYSO Crystals

Since the poor transmittance between 400 nm and 600 nm observed in SIPAT-LYSO-L7 reduces its light output it therefore should be eliminated. Similar poor transmittance was also found in other three LYSO samples of 20 cm long grown at SIPAT for a SuperB beam test: SIPAT-LYSO-L8, L9 and L10. Their longitudinal and transverse spectra were found to be similar to that shown in figures 5 and 6 respectively with poor transmittance located at the seed end. Poor

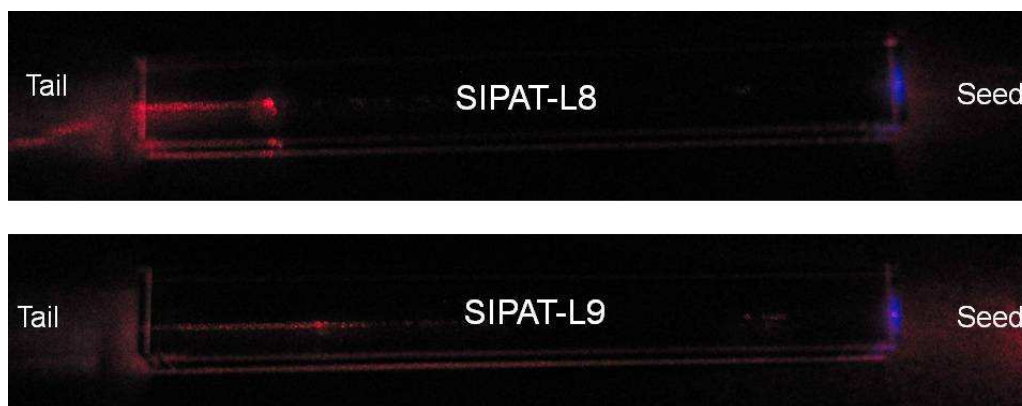


**Figure 8.** A picture showing scattering centers exists at the tail end of SIPAT-LYSO-L8 and SIPAT-LYSO-L9.

transmittance may be caused by point defects which absorb light in the crystal. It may also be caused by scattering centers introduced by macroscopic defects, such as cracking and inclusions etc. Scattering centers in a crystal may be observed by shooting a He-Ne red laser beam through the crystal. Figure 8 shows two photos for SIPAT-LYSO-L8 and SIPAT-LYSO-L9 with the laser beam entering longitudinally from the seed end (right) of the crystals. Scattering centers are clearly visible at the tail end of these crystals. Observations also show scattering centers at the tail end for other crystals with poor longitudinal transmittance. Since the poor transmittance was found at the seed end this observation ruled out macroscopic defects at the seed end. We thus conclude that the poor transmittance in these samples are caused by point defects at the seed end which absorb light.

This issue of the absorption band at the seed end found in SIPAT-LYSO-L7, L8, L9 and L10 was brought to the attention of SIPAT, and was discussed in a site visit. The problem was traced back to a bad seed crystal used in the growth process. After a rigorous quality control for the seed crystals the absorption band at the seed end was eliminated. Figure 9 show the longitudinal transmittance spectra for eleven LYSO crystals: ten from SIPAT and one from Saint-Gobain. No absorption was found between 400 nm and 800 nm for SIPAT-LYSO-L11 to L16, which were grown with seed crystals of high quality, and the Saint-Gobain sample. A specification of 75% at 420 nm was introduced to reject crystals with poor longitudinal transmittance. Because of the improvement in optical transmittance the light output of 20 cm long LYSO crystals from SIPAT is 30% higher than that with the absorption problem as shown in Table 1. The average

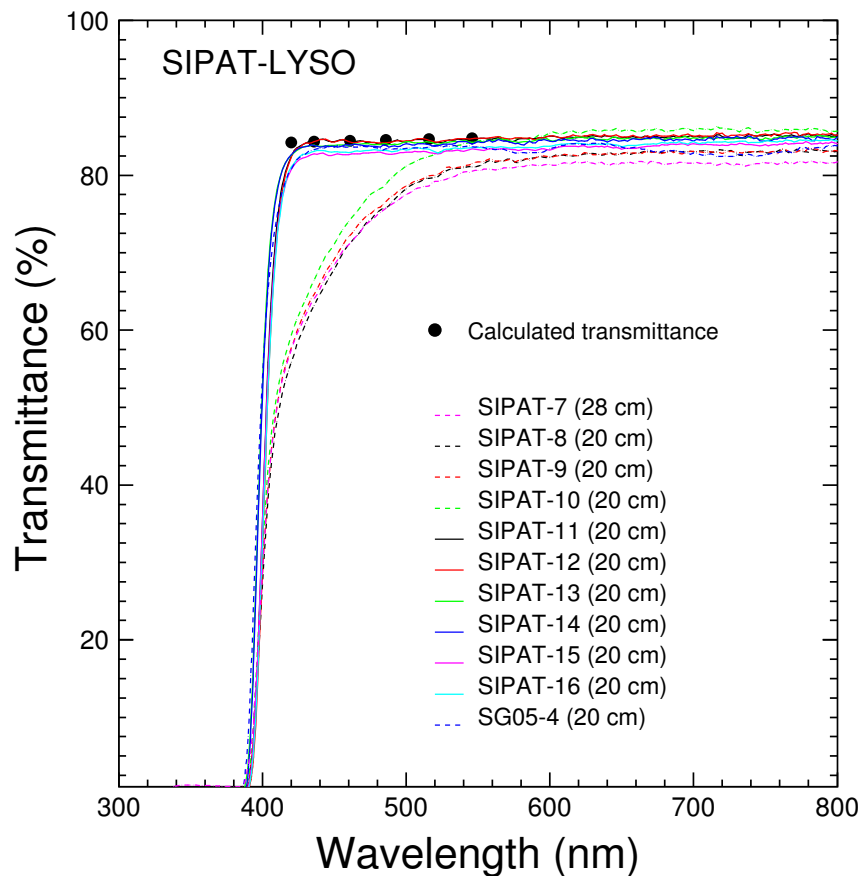


**Figure 9.** Longitudinal transmittance spectra are shown as a function of wavelength for eleven LYSO crystals: ten from SIPAT and one from Saint-Gobain.

FWHM resolution measured by the Hamamatsu R1306 PMT with 0.511 MeV  $\gamma$ -rays from a  $^{22}\text{Na}$  source for long LYSO samples have also been improved from  $>12\%$  to better than  $11\%$  as shown in Table 1.

**Table 1.** Light Output Measured with Hamamatsu R1306 PMT for SIPAT LYSO Samples

ID	Light Output (p.e./MeV)	Energy Resolution FWHM (%)
SIPAT-7	1380	12.2
SIPAT-8	1330	13.1
SIPAT-9	1450	12.3
SIPAT-10	1490	12.3
SIPAT-11	2010	10.7
SIPAT-12	1970	10.4
SIPAT-13	2050	11.5
SIPAT-14	2100	10.9
SIPAT-15	2040	10.5
SIPAT-16	2050	10.1

## 6. Summary

In a brief summary, LSO/LYSO crystals are an excellent material for a total absorption electromagnetic calorimeter for a future high-energy physics experiment in a severe radiation environment. The first  $2.5 \times 2.5 \times 28$  cm ( $25 X_0$ ) LYSO sample was successfully grown at SIPAT. It has consistent emission, adequate light response uniformity and good radiation resistance against  $\gamma$ -rays up to 1 Mrad. This sample and three other large size samples from SIPAT, however, showed poor longitudinal transmittance between 400 nm and 600 nm as well as poor transverse transmittance at the seed end. This poor transmittance at the seed end was understood as being caused by point defects which absorb light, and was traced back to a bad seed crystal used in their growth. With rigorous quality control on seed crystals recently grown LYSO crystals show no absorption band at the seed end and have a light output of 30% more than those with this problem. The corresponding average FWHM resolution measured by using 0.511 MeV  $\gamma$ -rays from a  $^{22}\text{Na}$  source is also improved from  $>12\%$  to better than 11%. Because of the crystals excellent radiation hardness, a LSO/LYSO crystal calorimeter is capable of making precision measurement for electrons, photons and jets and thus provides a great physics discovery potential in a severe radiation environment, like the HL-LHC.

## Acknowledgments

This work is partially supported by the U.S. Department of Energy Grant No. DE-FG03-92-ER40701 and the U.S. National Science Foundation Award PHY-0612805 and PHY-0516857.

## References

- [1] C. Melcher and J. Schweitzer, "Cerium-doped lutetium oxyorthosilicate: a fast, efficient new scintillator," *IEEE Trans. Nucl. Sci.* **39** (1992) 502–505.
- [2] D.W. Cooke, K.J. McClellan, B.L. Bennett, J.M. Roper, M.T. Whittaker and R.E. Muenchausen, "Crystal growth and optical characterization of cerium-doped  $\text{Lu}_{1.8}\text{Y}_{0.2}\text{SiO}_5$ ," *J. Appl. Phys.* **88** (2000) 7360–7362.
- [3] T. Kimble, M Chou and B.H.T. Chai, "Scintillation properties of LYSO crystals," in *NSS conference Record 2002 IEEE*, Vol 3, 1434–1437.
- [4] J.M. Chen, R.H. Mao, L.Y. Zhang and R.Y. Zhu., "Large size LSO and LYSO crystal for future high energy and nuclear physics experiments," *IEEE Trans. Nucl. Sci.* **54** (2007) 718–724.
- [5] C. Cecchi, A LYSO Calorimeter for the super B factory, 2011 J. Phys.: Conf. Ser. 293 012066.
- [6] F. Happacher, *CCALT: Crystal Calorimeter at KLOE2*, 2011 J. Phys.: Conf. Ser.
- [7] The Mu2e Experiment, see <http://mu2e.fnal.gov/>.
- [8] J.M. Chen, R.H. Mao, L.Y. Zhang and R.Y. Zhu, "Gamma-ray induced radiation damage in large size LSO and LYSO crystal samples," *IEEE Trans. Nucl. Sci.*, **54** (2007) 1319–1326.
- [9] Rihua Mao, Liyuan Zhang and Ren-yuan Zhu, "Effects of neutron irradiations in various crystal samples of large size for future crystal calorimeter," *2009 IEEE NUCLEAR SCIENCE SYMPOSIUM CONFERENCE RECORD*, VOLS 1-5 (2009) 2041–2044.
- [10] F. Nessi-Tedaldi, G. Dissertori, P. Lecomte, D. Luckey and F. Pauss, "Studies of Cerium Fluoride, LYSO and Lead Tungstate Crystals Exposed to High Hadron Fluences", Paper N32-3, 2009 IEEE NSS Conference.
- [11] J.M. Chen, R.H. Mao, L.Y. Zhang and R.-Y. Zhu, *IEEE Trans. Nucl. Sci.* **54** (2007) 718.
- [12] J.M. Chen, R.H. Mao, L.Y. Zhang and R.-Y. Zhu, *IEEE Trans. Nucl. Sci.* **54** (2007) 1319.
- [13] Rihua Mao, Liyuan Zhang and Ren-yuan Zhu, "Optical and Scintillation Properties of Inorganic Scintillators in High Energy Physics," *IEEE Trans. Nucl. Sci.* **55** (2008) 2425–2431.
- [14] D. A. Ma and R. Y. Zhu, "Light attenuation length of barium fluoride crystals," *Nucl. Instr. and Meth.* **A333**, (1993) 422–424.
- [15] Rihua Mao, Liyuan Zhang and Ren-yuan Zhu, "Gamma-ray induced radiation damage in PWO and LSO/LYSO crystals," *2009 IEEE NUCLEAR SCIENCE SYMPOSIUM CONFERENCE RECORD*, VOLS 1-5 (2009) 2045–2049.
- [16] R.H. Mao, L.Y. Zhang and R.-Y. Zhu, *Optical and Scintillation Properties of Inorganic Scintillators in High Energy Physics*, *IEEE Trans. Nucl. Sci.* **NS-55** (2008) 2425–2431.
- [17] D.A. Ma and R.-Y. Zhu, *Nucl. Instr. and Meth.* **A333** (1993) 422.